

On the Coordination of Actinides and Fission Products in Silicate Glasses

Amine Haddi¹, François Farges^{1,2,3}, Patrick Trocellier⁴, Enzo Curti⁵,
Messaoud Harfouche¹, and Gordon E. Brown^{3,6}

¹ Laboratoire des Géomatériaux, Université de Marne-la-Vallée, France

² USM 201 « Minéralogie-Pétrologie », Muséum National d'Histoire Naturelle, CNRS UMR 7160, Paris, France

³ Department of Geological and Environmental Sciences, Stanford University, USA

⁴ Service de Recherches de Métallurgie Physique, CEA, Saclay, France

⁵ Waste Management Laboratory, Paul Scherrer Institut, Switzerland

⁶ Stanford Synchrotron Research Laboratory, Menlo Park, USA

Abstract. The local structure around Th, U, Ce and Nd in leached silicate glasses was examined using XAFS spectroscopy at their L₃ edges and also at the K edge of Fe, Co, Ni, Zr and Mo. Pellets of inactive borosilicate glasses with a simplified or a complex composition were leached statically at 90°C, at pH buffered to 0 or 6 for 28 days (surface/volume, S/V, ratios of 0.1 cm⁻¹). These glasses are compared to another SON68 sample (denoted “SP1” in this paper) that was statically leached for 12 years under similar conditions, except for a higher S/V of 12 cm⁻¹ and a higher unconstrained pH of 9.6. The speciation of Fe, Co, Ni, Zr and Mo in the simple and the complex unleached are similar. In the statically leached glasses, the speciation of these transition metals is mostly identical to in the unleached glasses, except in the gels formed at the surface of the glasses leached at low pH, where large speciation differences are observed. Surface precipitates, especially for Fe (as ferrihydrite), Mo (possibly sidwillite) and Th (as ThO₂) were detected. Finally, the drying of the gels considerably affects the metal speciation by enhancing metal polymerization.

Keywords: nuclear glasses, leaching, redox, XAFS spectroscopy.

PACS: 61.43.Fs, 61.10.Ht, 28.41.Kw, 21.60.Jz

INTRODUCTION

The long-term durability of oxide glasses is a crucial issue because these materials are designed as matrices to host a variety of toxic and/or radioactive ions (e.g., transition elements, such as Co, Ni, Ce, Zr, Mo, as well as natural and artificial actinides) [1-5]. In this study, the aqueous corrosion of waste glasses for nuclear storage is investigated by tracing, using XANES spectroscopy, speciation changes around these elements before and after leaching. These elements were selected because they represent a wide range of cations and network modifying structural positions in nuclear glasses, typical of divalent (Co, Ni), trivalent (Fe, Ce), tetravalent (Zr, Ce, Th) and hexavalent (Mo, U) cations.

EXPERIMENTAL

Three types of borosilicate glasses were studied. First, a series of simplified sodo-calcic

aluminoborosilicate compositions that mimic more complex nuclear borosilicate glasses were synthesized with or without additional Fe (3 wt.%), Mo (1.7 wt.%), and Ce (5 wt.%) to investigate the influence of these cations on leaching (see [6] for details on sample chemistry). Second, more complex compositions, closer to the actual nuclear waste glass used in France, were studied. They include the so-called “M”, “F” and “SON68” compositions (detailed compositions are in [6]). “F” and “M” glasses are test compositions, whereas SON68 simulates more closely the R7T7 composition but without artificial actinides and their fission products. These glasses were cut to form pellets (\varnothing 200 µm, thickness = 2 mm; surface/volume ratio, S/V, = 0.1 cm⁻¹) and set in a Teflon container for static leaching during 28 days at pH buffered to 0 or 6 and 90°C. These glasses were previously investigated using ion-beam analyses (RBS, ERDA, PIXE, PIGE [4,6]). Third, we investigated another sample of SON68 composition from Marcoule (labeled “SP1”) leached at the Paul Scherrer Institut (Switzerland) for more than 12 years, also under static conditions at

90°C and unconstrained pH 9.6 (in stainless steel vessels) [7]. Its specific surface area is 0.030 ± 0.002 m^2/g ; S/V $\sim 120\text{-}0 \text{ m}^{-1}$). X-ray absorption near edge structure (XANES) spectra were collected at the 11-2 beamline (SSRL, Stanford, USA). High energy resolution (0.6 eV at the Fe-K edge) XANES spectra were collected using a Si(220) double-crystal monochromator. A “Lytle” detector was used to collect the K_α fluorescence from Fe, Co, Ni, Zr and Mo and the L_α/β fluorescence from Ce, Th and U. The spectra were normalized using conventional methods (“xafs” package [8]) as detailed in [9-10]). Due to the μm -scale thickness of these leached layers, no EXAFS could be collected for the leached samples.

RESULTS AND DISCUSSION

Actinides and Rare-Earths

Figure 1 shows the normalized XANES spectra collected at the U-L₃ edge for the SON68 glass and its leached equivalent SP1 (2 spots probed). The energy position of the XANES spectra indicates that U is hexavalent in both glasses. Because feature B increases in intensity in SP1 as compared to in SON68, an increase in the contribution from axial U-O oxygens is then observed due to leaching (see [10]). No other change is detected due to leaching. At the Th-L₃ edge (Fig. 2), the XANES spectra for the unleached glass “M”, its fresh gel and its dried counterpart show more changes, esp. in features A and B. Feature A is present in the hydrous gel, as in ThO_2 , indicative of Th-Th pairs [11]. Changes in feature B position are due to changes in average Th-O distance, suggesting that drying is affects the local structure around Th. Figure 3 shows the Ce L₃-XANES for two unleached glasses, with and without Th. No influence of the composition is observed on the speciation of Ce, which is a mixture of Ce(III) and Ce(IV). Similarly,

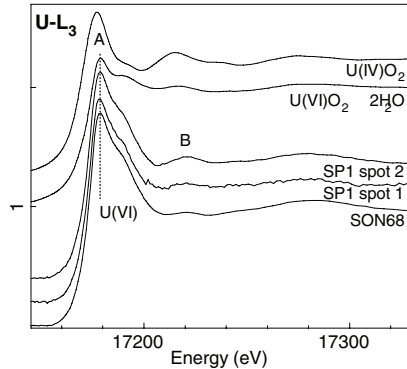


FIGURE 1. U L₃-edge XANES spectra for the fresh SOM68 and leached SP1 (2 different areas probed).

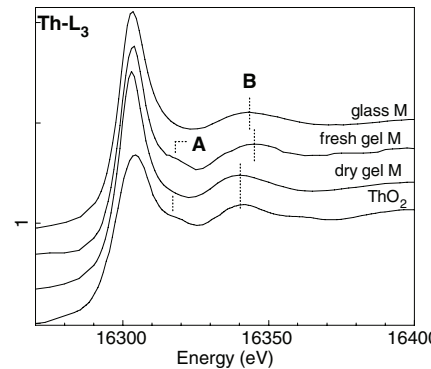


FIGURE 2. Th L₃-edge XANES spectra for the glass M, its gel (hydrous and dried), as compared to ThO_2 model.

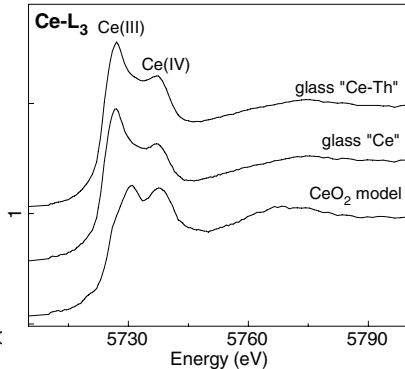


FIGURE 3. Ce L₃-edge XANES spectra for 2 unleached glasses studied as compared to CeO_2 model.

Nd(III) does not show significant change in speciation for the various glasses studied (data not shown).

Iron, Cobalt and Nickel

The Fe K-edge XANES spectra (Fig. 4) are shown for various unleached glasses, as well as for the hydrous gels formed on glasses M and SON68 and, finally, for the leached SOM68 (SP1) glass. All non-leached glasses show comparable Fe K-edge XANES. Their pre-edge feature is close to that for Fe:LiAlO₂, in which iron is trivalent and tetrahedrally coordinated [8]. In SP1, the same features are observed as in SON68, indicating no detectable structural changes due to leaching. The Fe K-edge XANES (including its pre-edge feature A) for the gel of the leached “M” glass resembles that of ferrihydrite (Fe(OH)_3). Figure 5 shows the Co K-edge XANES spectra collected for various model compounds of Co(II) and Co(III) as well as for the unleached SON68 and SP1 glasses. The Co K-edge (feature B) position for SON68 is close to that for Co(II) model compounds, indicating that Co is dominantly divalent in that glass. Further, the first EXAFS oscillation (feature C) is shifted to higher energies in the glass, indicative of the presence of lower average Co(II)-O distances as compared to 6-coordinated Co(II) in Co(OH)_2 . This is consistent with the presence of tetrahedrally coordinated Co(II) in SON68, as observed in other silicate glasses [11]. In SP1, the same features are observed as in SON68. Figures 6 and 7 show the Ni K-edge XANES and their pre-edge feature (labeled A) collected for model compounds and the glasses SON68 and SP1. These XANES are typical of Ni in an average symmetry (C_{3v}) close to that encountered in KNiPO_4 , in which Ni(II) is 5-fold coordinated (Fig. 7). As for U, Fe and Co, the Ni K-edge XANES spectrum for SON68 and SP1 samples are unaffected by the 12 years leaching.

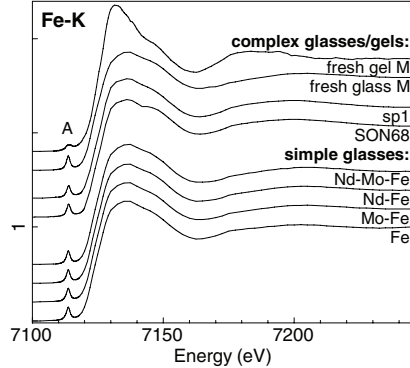


FIGURE 4. Fe K-edge XANES spectra for the fresh and leached glasses.

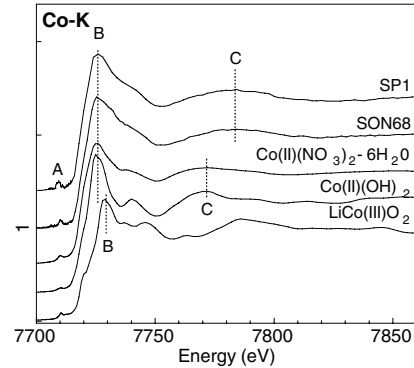


FIGURE 5. Co K-edge XANES spectra for 3 models (bottom) and 2 glasses.

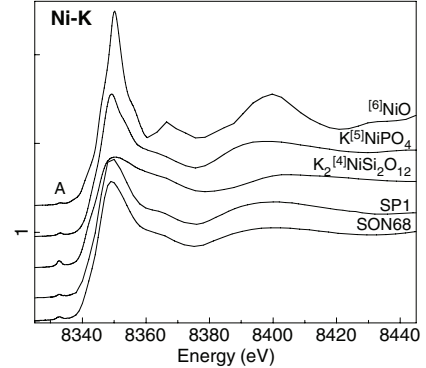


FIGURE 6. Ni K-edge XANES spectra for the unleached and leached glasses.

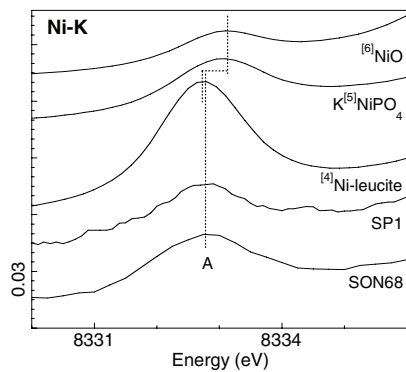


FIGURE 7. Detailed view of the pre-edge region shown in Fig. 6.

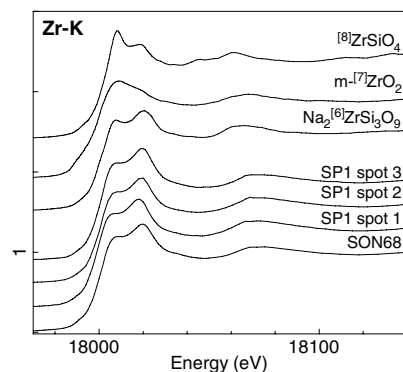


FIGURE 8. Zr K-edge XANES spectra for 3 models (top curves) and glasses.

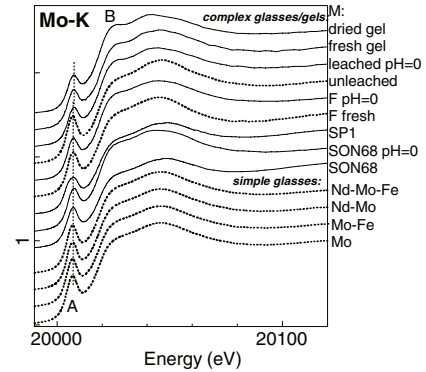


FIGURE 9. Mo K-edge XANES for unleached (dotted) and leached glasses.

Zirconium and Molybdenum

Figures 8 and 9 show the normalized Zr and Mo K-edge XANES for SON68 and SP1 glasses. No structural changes are observed in the leached SP1 sample as compared to its unleached “analog” SON68. The Zr K-edge XANES spectra for both glasses are typical of 6-fold coordination, whereas the Mo spectra suggest the presence of $\text{Mo(VI)}\text{O}_4^{2-}$ moieties. Further, the Mo K-edge XANES for the unleached glasses of the “simple composition” are similar to those of the complex SON68 and SP1 compositions. As compared to these glasses, the Mo K-edge XANES spectrum for the non-dried gel (formed on glass M) shows a less resolved pre-edge feature (A). This suggests the presence of 6-fold coordinated Mo(VI) [10]. Slow drying of this gel (after a couple of hours) enhances the main XANES features, indicative of ordering around Mo in the gel through removal of hydroxyls.

CONCLUSIONS

At the mm scale probed here, static leaching has few noticeable effects on the speciation of the cations investigated here, even after 12 years. This is probably due to the very thin alteration rims (a few μm , see [7])

formed under the selected mild alteration conditions. However, speciation changes are noteworthy on the gels formed under more “aggressive” conditions. For Mo and Fe, metal-rich oxide-type compounds precipitate in the gel, which is consistent with other observations for Zr, Fe, Ce and U [12-14]. Finally, metal polymerization increases with time in the gels studied, especially upon drying (as observed for Mo and Th), so the study of gels *in-situ* is important.

REFERENCES

1. S.R. Gislason, H.P. Eugster, *Geochim. Cosmo. Acta* **51**, 2827 (1987).
2. J.-L. Crovisier *et al.*, *Appl. Clay Sci.* **7**, 47 (1992).
3. E. Vernaz *et al.*, *J. Nucl. Mater.* **298**, 27 (2001).
4. P. Trocellier *et al.*, *Nucl. Instr. Meth. Phys. Res. B* **240**, 337 (2005).
5. J. A. Fortner *et al.*, *Ultramicroscopy* **67**, 77 (1997).
6. A. Haddi *et al.*, *Nucl. Instr. & Meth. B* (in press) (2006).
7. E. Curti *et al.*, *Appl. Geochem.* **21** (2006) 1152–1168,
8. M. Winterer, *J. Phys. IV France* **7**, C2 – 243 (1997).
9. F. Farges *et al.*, *J. Non-Crystall. Sol.* **344**, 176 (2004).
10. F. Farges *et al.*, *Geochim. Cosmo. Acta* **56**, 4205 (1992).
11. G.E. Brown Jr. *et al.*, *Rev. Mineral.* **32**, 317 (1995).
12. P. Jollivet *et al.*, *J. Nucl. Mater.* **301**, 142 (2002).
13. P. Jollivet *et al.*, *J. Nucl. Mater.* **346**, 253 (2005).
14. E. Pelegrin *et al.*, *J. Am. Ceram. Soc.* **82**, 2219 (1999).